Indian Journal of Geo Marine Sciences
Vol. 50 (03), March 2021, pp. 193-202

Wave attenuation by coastal heterospecific vegetation - modeling of synthetic plant meadows by Response Surface Methodology (RSM)

S Hemavathi* & R Manjula
Department of Civil Engineering, National Institute of Technology, Tiruchirappalli (NITT), Tamil Nadu – 620 015, India
*[E-mail: 403116005@nitt.edu]

Received 21 October 2019; revised 20 March 2020

Knowing the interactions between wave and aquatic vegetation is becoming increasingly important because of the phenomenon of plant-induced wave attenuation for the development of sustainable coastal management systems. Many of the wave-vegetation interaction studies focus on monotypic coastal plant meadows, while coastal plant meadows are typically heterospecific in nature, and the work on heterospecific plant meadows is still very limited. This research aims therefore to explain the heterospecific vegetation-wave interactions using a three-level four-factor surface response methodology (RSM) using controlled laboratory wave flume conditions. Heterospecific seagrass species, Cymodocea serrulata is physically simulated using synthetic plant mimics to establish a relationship between wave attenuation (E%) and four direct control factors, *i.e.* wave period (T), water depth (h), bed roughness factor (f) and plant density (N), using an empirical model. The model developed was evaluated using the methodology of variance analysis (ANOVA) and analyzed for the key and interaction effects of the parameters studied. The findings showed that both individually and in combination, all the parameters considered are significantly successful on E%. All model-based findings were compared with a new collection of experimental data, and validation tests were carried out.

[**Keywords**: Empirical modeling, Flume study, Response surface methodology (RSM), Wave-vegetation interactions]

Introduction

The rise of sea levels and decline of land surface along densely populated coastline is recognized by several nations across the world as a major threat for coastal areas. Native coastal ecosystems including seagrasses, salt marshes and mangrove forests[1–5] provide a broad spectrum of ecological resources and functions like foreshore vegetated structures[6,7]. Such habitats theoretically mitigate the effect of tides and waves at locations placed in front of constructed flood control systems. Local hydrodynamic climate is known to impact vegetated foreshore structures[8]. They serve as an interface between oceans and dry land, minimize wave height, form mixing layers[9] and regulate turbulence intensity due to several deeper water breaking waves and plant induced wave attenuation. This natural trend has contributed to the idea of sustainable coastal protection using a natural coastal defense network of seagrass meadows, salt marshes, and mangrove forest. With an ever-growing population and infrastructure alongside low-lying coastal areas, coastal vegetation's ability serves as a bio-shield or non-intrusive buffer to mitigate the combined effects of the rise in sea levels, and subsidence is recently a increased concern[10].

The interaction between wave-vegetation is complex, since not only does water flow affect the vegetation and vice versa, but both can interact in highly coupled, nonlinear ways[11]. Attenuation of a vegetation-caused wave is defined by the force exerted on the flowing water by the plants. According to Newton's third theorem, water concurrently exerts on plants a force of equal magnitude and direction opposite. Plant versatility defines how plant and wave motion interact and the degree of drag forces[12,13].

The level of attenuation relies on plant features such as plant height, plant rigidity, buoyancy, degrees of freedom, plant density, spatial structure, and hydrodynamic wave parameters such as wave height, water depth, wave period, speed, etc. The variation in wave damping is so high that a general normative method for controlled experiments on "plant-induced attenuation" is not yet well developed[14]. There is often either a lack of awareness due to the many varieties of vegetation associated with the different climatic conditions and their unique characteristics, or the insufficiency of modeling tools that allow vegetation to be taken into account[15].

Several field-based studies calculate wave attenuation by vegetation[16–19], laboratory flume

measurements[3,15,20-23], and computational models[9,14,24-26]. Wave magnitude attenuation depends on hydrodynamic variables such as wave height[27,28], wave period[29] and water depth[30] and vegetation properties such as root diameter, height, density[30,31] and flexibility[32,33]. Nearly all the available studies in literature refer to monotypic aquatic meadows of plants. Rather little research on heterospecific vegetation meadows has been recorded though it is well known[34] that each species of seagrass may occur as a heterospecific seagrass bed, an intermix with the other species. This knowledge is especially important for the tropical shore regions, where many seagrass species occur together in one meadow. Changes in mechanisms of wave-vegetation due to the structural complexity of the heterospecific meadow involving different species of seagrass are equally important, which invites attention from the scientific community to pursue its viability for achieving a sustainable coastal system.

In addition, the large number of independent processes control parameters involved, the impact of seagrass bed characteristics comprising different species of seagrass on wave attenuation is not easy to analyze. Therefore, a study involving heterospecific species in tropical environments is of particular interest. Within this study, an empirical model based on experimental design for wave transformation over underwater heterospecific vegetation (*Cymodocea serrulata*) is built within a laboratory flume. For the analysis, a three-level, four-factor central composite design based surface response methodology (RSM) was chosen. The objectives were to a) identify and select the control parameter operating limits for primary laboratory flume experiments, based on RSM; b) build a mathematical model to evaluate the impact of each of the selected process parameters on wave attenuation processes while determining their main and interaction effects and c) to compare and validate the predicated model results with a new collection of planned secondary experimental data.

Materials and Methods

Theory

The generalized equation of continuity within the aquatic vegetation is given by:

$$\frac{\partial u}{\partial x}+\frac{\partial w}{\partial z}=0 \quad \ldots (1)$$

Kobayashi *et al.*[35] derived an empirical method for monochromatic small-amplitude attenuation of the wave over submerged vegetation. By using the concept of momentum conservation an expression is given on the reduction of wave height by an exponential function:

$$\frac{H(x)}{H_0}=e^{-K_i\,\Delta x} \quad \ldots (2)$$

Where, K_i is the coefficient of the wave decay, H(x) is the wave height along with the canopy of vegetation; H_o is the wave height in front of the canopy tip, and Δx, the separation width.

Augustin et al.[20] performed hydraulic tests to assess wave height drop using rigid, elastic cylindrical dowels. Similar technique established by Dalrymple et al.[36] was used to evaluate wave height drop in a three-density vegetation field that differed along the line of wave movement. Mullarney & Henderson[37] used the principle of cantilever beams to derive a model from modeling plant movement due to wave forces. The proposed theory was compared with the motions of a particular species in a real aquatic vegetation meadow and was effectively demonstrated with a single parameter tuning. Also developed was a wave height attenuation formula that involves plant motion. For linear waves, the general wave height measurement formula is given when converted to energy density (E) as:

$$E=\frac{1}{8}\rho g H^2 \quad \ldots (3)$$

Where, ρ is seawater density, g is gravitational acceleration, and H is wave height. Fonseca & Cahalan[38], the reduction in wave energy density was measured using a percentage drop in energy density (E%) across a test section of 1m is given by:

$$E\%=\left[\left\{\frac{E(in)-E(out)}{E(in)}\right\}\times 100\right] \quad \ldots (4)$$

Where, E(in) is the energy density entering the 1 m test portion, and E(out) is the energy density that exits the 1 m test section.

Wave flume set up

The tests were performed in wave flume at the hydraulic laboratory, National Institute of Technology, Tiruchirappalli (NITT), Tamil Nadu, India. The wave flume is 12.5 m in length, 0.3 m in width and 0.6 m in depth, and is fitted with a piston type wave generator on one side of the flume. To prevent wave reflection, rubble masonry wave absorber with 1:7 aspect ratio was installed in the

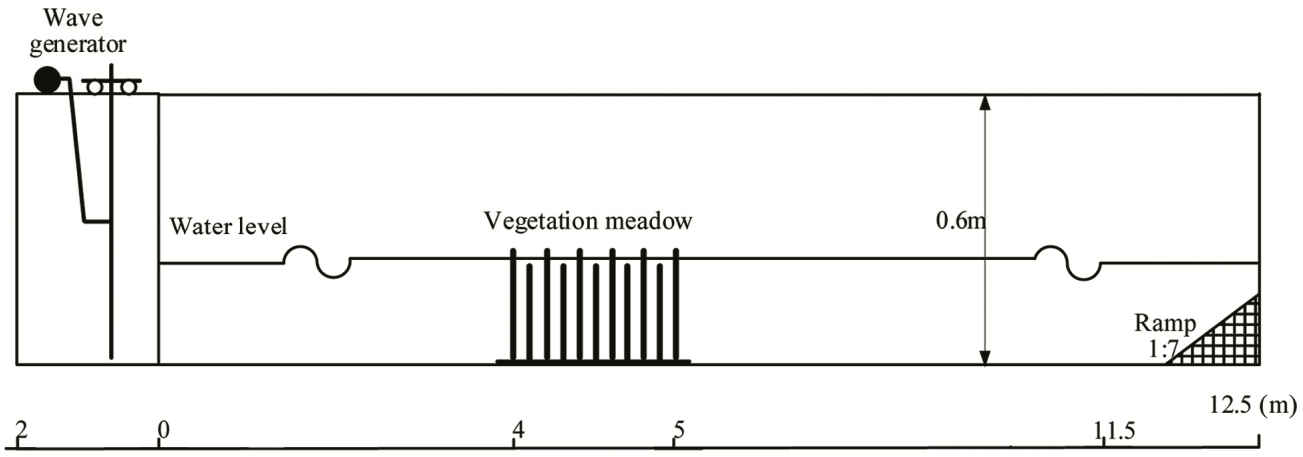

Fig. 1 — Details of the experimental setup

wave generator's opposite direction. A heterospecific artificial plant meadow was established in the middle portion of the flume, as shown in Figure 1. The meadow started about 4 m away from the wave paddle.

Heterospecific Cymodocea serrulata meadow conditions

Cymodocea serrulata is a coastal seagrass plant with roots, stems and leaves, forming thick vegetative colonies primarily in shallow estuaries[39,40]. It has a smaller leaf structure with tufts or whorl-like blades that distinguish it from other seagrass species. India's seagrasses contains 14 populations of about 50 species from seven genera worldwide[39]. The Gulf of Mannar and Palk Bay are predominantly situated in the southeast coastal regions as well as the island lagoons of Lakshadweep in the Arabian Sea and the western portion of Andaman and Nicobar in the Bay of Bengal in eastern India.

The physical properties of selected plants are important for studying wave interactions, leaf bends and the resulting efficiency of wave damping, such as density and rigidity. In the current research, artificial polypropylene models are chosen on the basis of the most similar physical characteristics to real leaves such as the elasticity modulus E = 0.9 GPa in the Cymodocea serrulata meadow (Figs. 2a & b). For a typical natural Cymodocea serrulata with 4-5 leaves, 1 cm (100-200 mm long and 3-5 mm wide) stems may be mounted in opposite directions with lengths up to 100 and 150 mm.

Artificial polypropylene plants of the Cymodocea serrulata have a diameter of 0.005 m and length of leaves with polypropylene streaks is 100 mm and 150 mm (Figs. 1 & 2). Each simulated plant has four

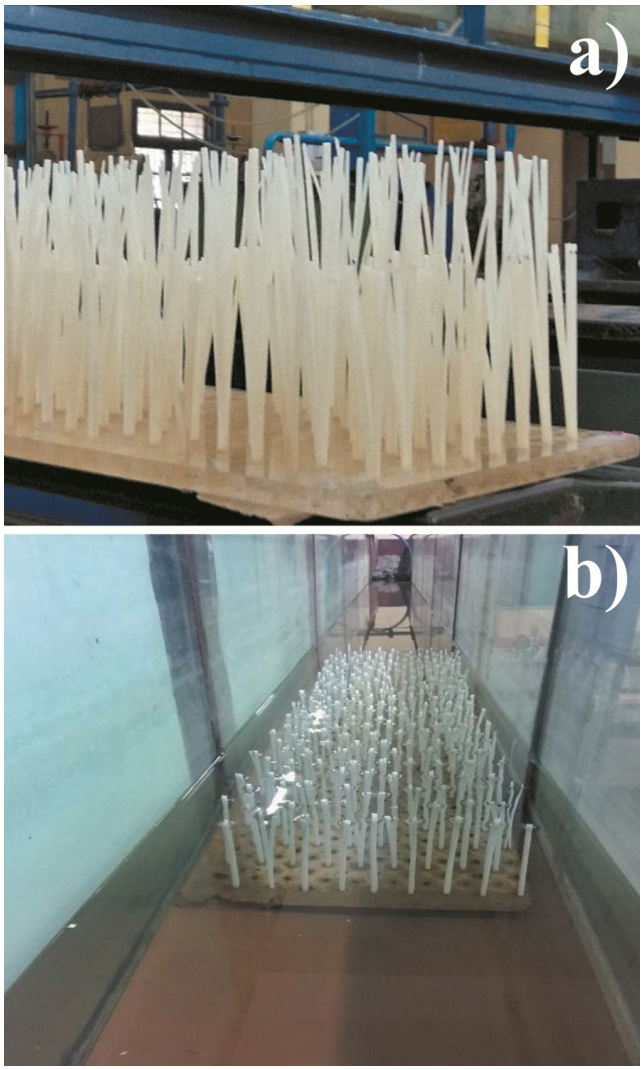

Fig. 2 — (a) Morphological characteristics used to study plant species in synthetic form; and (b) The plant species mimics in the flume under evaluation

leaves attached to a stem of 10 mm. The mimics were installed on a standard 1000 mm and 260 mm acrylic base frame and connected to a staggered distribution with a width of 43 mm to retain the plant density of 543 stems/sq m. Likewise; a spacing of 21.5 mm was maintained to achieve a plant density of 2163 stems/sq m. SONY, Model No: 25Hz HDR-PJ50V has recorded both the experiment and the wave profiles. The recorded video images were analyzed using MATLAB image processing system and the wave profile time series was collected. Wave height was used before and during wave attenuation.

Central composite design (CCD)

Experiment design was a commonly used, effective, statistical approach for designing experiments, based on second-order multivariate models. The present study uses a typical RSM design termed Central Composite Design (CCD) model to analyze regression model equations from the collected data. The regression equations developed are useful in studying the input parameter interactions which affect the process. Valid and objective conclusions are drawn from the regression equations analysis to ensure the experiments are efficient. It is also useful to research the interactions of the different parameters that affect the operation.

The Design of Experiment (DOE) process started with the identification of the input variables and the output (response) to be calculated followed by three main execution steps: (1) discovery, preparation and execution of the most appropriate statistically designed experiments; (2) creation of a mathematical model by estimating the coefficients, and (3) analysis and predicting the answer and test the model's appropriateness[41]. The RSM technique involves creating a connection between the variables k by a polynomial expression of the second order. The real relationship among independent control factors or x_1, $x_2 ... x_k$ and response Y (dependent variable) can be expressed as follows:

$$Y = f(x_1, x_2, ..., x_k) \quad \ldots (5)$$

Where, 'f' is a system's unknown true response. For RSM, the most common model is the polynomial to establish an estimated relationship between variables and response functions through a systematic sequence of experiments and statistical analysis. The second non-linear polynomial equation is given in the following equation[41].

$$Y = \beta_0 + \sum_{i=1}^{k} \beta_i x_i + \sum_{i=1}^{k} \sum_{j=1}^{k} \beta_{ij} x_i x_j + \sum_{i=1}^{k} \beta_{ii} x_{ii}^2 + \varepsilon \quad \ldots (6)$$

Where, the predicted response is given as Y (wave attenuation performance, in this case E(%); X_i and X_j are the independent coded variables; k is the number of variables, β_0 is the model term constant; β_i, β_{ii}, β_{ij} is the direct, square and interaction effect respectively, and ε is the random experimental error. Face-centered Central Composite Design (FCCD) method has been used for the present study. Based on the results of an earlier study, four main variables, wave period (T), water depth (h), bed roughness factor (f), and plant density (N) were selected along with the three levels of each variable with "-1," "0" and "+1" representing low, medium and high factor levels, respectively as shown in Table 1. The experiments used steel surface, fine sand, and coarse pebbles to reflect the low (-1), middle (0) and high (+1) bed roughness levels, respectively. By design, the FCCD method needs 30 experimental runs and, with 3 replications, a total of 90 experiments were conducted at random to remove systematic errors. Statistical software (Minitab ® software release 17) was used for the statistical analysis of the experimental data and their response surface graph. Regression analysis was carried out on the data collected to assess the attribution effects on the expected response of the selected variables, E%. Constructed with plastic as a series of modules on board, the simulated seagrass meadow for Cymodocea serrulata was fixed firmly together and to the floor of the flume. Between the flume walls and the meadow there was sufficient gap to allow free movement of plant mimics so that the actual dispersion of the

Table 1 — Original and coded values of control variables

Control variables	Unit	Notation	Coded symbol	The original value of coded levels		
				-1	0	+1
Water depth	m	h	β_1	0.10	0.125	0.150
Wave period	s	T	β_2	1.0	2.0	3.0
Plant density	stems/sq m	N	β_3	543	1353	2163
Bed roughness factor	-	f	β_4	0.010	0.017	0.025

seagrass meadow in shallow waters could be better represented[34].

Results and Discussion

Tables 2 and 3 detail the architecture matrix for the repeated experimental outcomes and the data collected. Statistical software has been used to: a) research experimental data regression analysis; b) suit a non-linear quadratic model, and c) draw plots of the response surface. The statistical parameters were calculated using a method called ANOVA (variance analysis). The empirical model developed is shown in equation (7) as a coded factor for predicting E%:

$$Y = \beta_0 + \beta_1 h + \beta_2 T + \beta_3 N + \beta_4 f + \beta_{1,2} h\, T + \beta_{1,3} h\, N + \beta_{2,3} T\, N + \beta_{2,4} T\, f \ldots + \beta_{1,1}(h)^2 + \beta_{2,2}(T)^2 + \beta_{3,3}(N)^2 + \beta_{4,4}(f)^2 \quad \ldots (7)$$

Where, β_0 is the average of the responses and $\beta_0, \beta_1, \beta_3, \ldots, \beta_{44}$ are the regression coefficients that depend on corresponding linear, interaction, and quadratic terms of the factors[41]. Using the program, the value for each coefficient was determined. Table 2 provides the results of the regression coefficients for the second-order surface response model. The final empirical model has been built using these coefficients given in equation (8) below:

$$E\% = 52.80 - 21.56h - 14.24T + 2.49N + 5.44f + 15.27\, h * T - 6.29h * f + 3.20T * f - 11.93(T)^2 + 15.40(N)^2 - 25.11(f)^2 \quad \ldots (8)$$

ANOVA is used for checking the adequacy and statistical significance of the quadratic model built for response (E%). The findings are listed in Table 3. For the established quadratic model, the coefficient of multiple determination (R^2) is found to be greater (0.988) which means that the model cannot mean only a total variation of 0.012. Failure to match the F-value for the model was found to be 5.00 (not shown in the table) indicating substantial lack of fit. Owing to noise this large value may occur. In fair accordance with the modified R^2 value of 0.976 the expected R^2 value is 0.944. The proper precision value calculates the ratio of the signal to the noise. It is important to get a ratio greater than 4.2. The ratio of 25 indicates an adequate signal for the present model, and thus this established model can be used to traverse the design room. A new series of experiments under identical experimental conditions were performed for validation of the

Table 2 — Estimated regression coefficients

Factor	Estimated coefficient
Intercept	52.80
h	-21.56
T	-14.24
N	2.49
f	5.44
h^2	-1.52
T^2	-11.93
N^2	15.40
f^2	-25.11
h*T	15.27
h*N	-1.36
h*f	-6.29
T*N	-0.57
T*f	3.20
N*f	0.083

Table 3 — ANOVA test results for E(%)

Source	Sum of Squares	df	Mean square	F_p Value	p-value Prob > F_p	Remarks
Regression	22041.05	14	1574.36	85.87	< 0.0001	Significant
h	8370.02	1	8370.02	456.53	< 0.0001	Significant
T	3650.00	1	3650.00	199.08	< 0.0001	Significant
N	112.05	1	112.05	6.11	0.0259	Significant
f	532.47	1	532.47	29.04	< 0.0001	Significant
h^2	6.02	1	6.02	0.33	0.5751	
T^2	368.71	1	368.71	20.11	0.0004	Significant
N^2	614.11	1	614.11	33.50	< 0.0001	Significant
f^2	1633.52	1	1633.52	89.10	< 0.0001	Significant
h*T	3728.93	1	3728.93	203.39	< 0.0001	Significant
h*N	29.38	1	29.38	1.60	0.2249	
h*f	633.28	1	633.28	34.54	< 0.0001	Significant
T*N	5.29	1	5.29	0.29	0.5990	
T*f	164.22	1	164.22	8.96	0.0091	Significant
N*f	0.11	1	0.11	0.006	0.9396	
Pure Error	68.84	5				
Cor Total	22316.06	29				

R^2(Adequate) = 98.77 %, R^2(Adjusted) = 97.62 %, R^2(Predicted) = 94.37 %, df - degrees of freedom, Fp - Fisher's ratio, and p - probability

existing regression model. The data collected was plotted against the results provided from the regression model being developed and is shown in Figure 3. Every expected value from the established model correlates well with its newly generated experimental value.

The high F value (52.80; Table 2) and the corresponding lower p-value (less than 0.0001, Table 2) suggest that the terms of the model and function are statistically important for the regression model being created. The influence of p-value-related terms greater than 0.05 on the model is statistically negligible. In this scenario, it is observed from Table 3 that all the linear terms of h, T, N and f; the quadratic terms of $(T)^2$, $(N)^2$ and $(f)^2$ along with the interaction terms of (h)×(T), (h)×(f) and (T)×(f) are critical to the response, E%. The quadratic terms of $(h)^2$ and the interaction term of (h)×(N), (T)×(N) and (N)×(f) have negligible consequences (Factors listed in Table 2). The sensitivity degree of significant terms for E% from largest to the least is the linear term of h, T, N and f, the quadratic term of $(N)^2$, $(T)^2$, $(f)^2$ and the interaction term of (h)×(f). The linear term is thus the most important, the interaction term is the second most significant, and the quadratic term is less important for the E%. These statistical results clearly indicated that the water depth h has a definite linear relationship with f while T has a nonlinear relationship on wave attenuation.

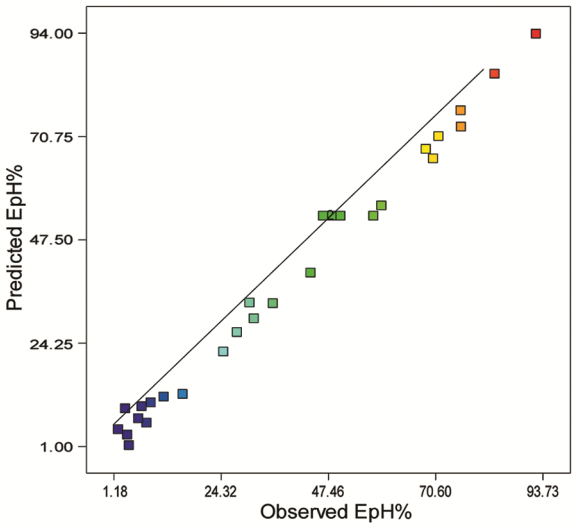

Fig. 3 — Comparison between predicted and experimental E%

Parameter effects

The findings from the probability value f F-statistics (p less than 0.05), suggested that the model built in equation (8) might draw a strong correlation between input and output variables. Parametric variables h, T, N, and f independently play a significant role in vegetation-induced wave attenuation. The graphical representation of the major effects of statistically significant factors with their respective model-based magnitude and direction of regression on response (E%) is shown in Figure 4(A-D). This shows that h and T have inverse effects among the linear coefficients, and that N and f have direct effects on E%. It is well known that under steady flow conditions, vegetational attenuation depends on plant characteristics such as plant morphology, densities, meadow size, mechanical properties particularly rigidity and buoyancy and hydro-dynamics like wave height, water depth and wave period[27]. The findings of this research are in strong alignment with the majority of laboratory-based flume, field and simulation studies supporting the reliance of wave-vegetation interactions on water depth (h)[2,27,38], wave period (T)[16,27,29,37], plant density (N)[12] and bed roughness factor $(f)^2$. Overall, surface wave attenuation is induced by the drag (energy

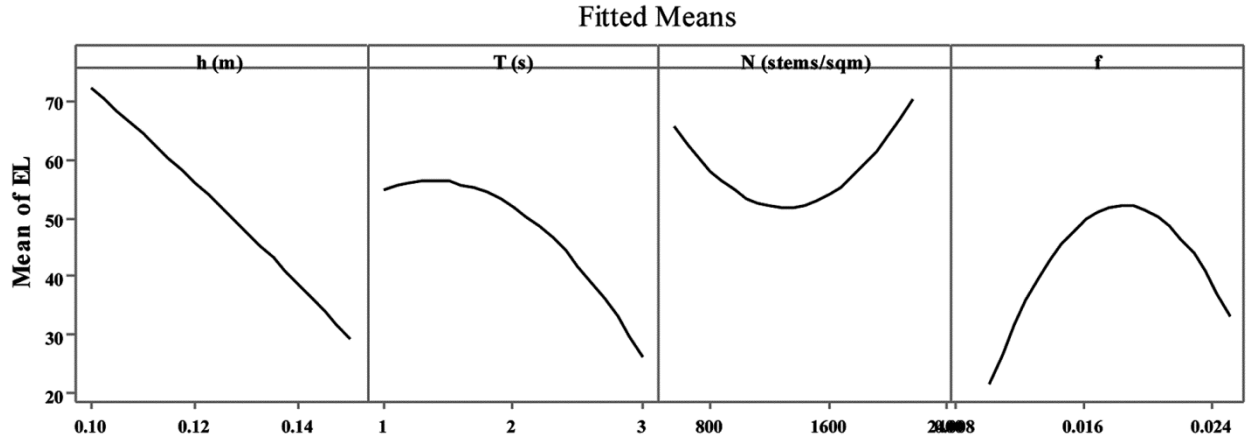

Fig. 4 — The main effect of model parameters on E%

loss) of both emerging and submerged vegetation stems.

Interaction effects of model parameters

The interaction results of all statistically significant control variables on E% over vegetation meadow are shown graphically in the following sections. The plots demonstrating the two-way interaction effect between the four parameters considered for wave attenuation are as follows: h-T (Fig. 5) and T-f (Fig. 6) direct relationship; and h-f (Fig. 7) inverse relationship. Since linear effect of h and quadratic effect of T, N and f are significant, these will serve as restricting parameters and the minor variance in their rates will also significantly alter the E%.

Interaction effect between h and T

Figure 5(a & b) show h and T' with E% association over the vegetation field. For a plant stem density N (1353 stems/sq m), and a friction factor f (0.0175), E% is plotted here. At lower h (0.10 m) and T (1.0 s), E% is maximum (92 %) and rise in h have resulted in a decrease in energy loss as waves moved along the

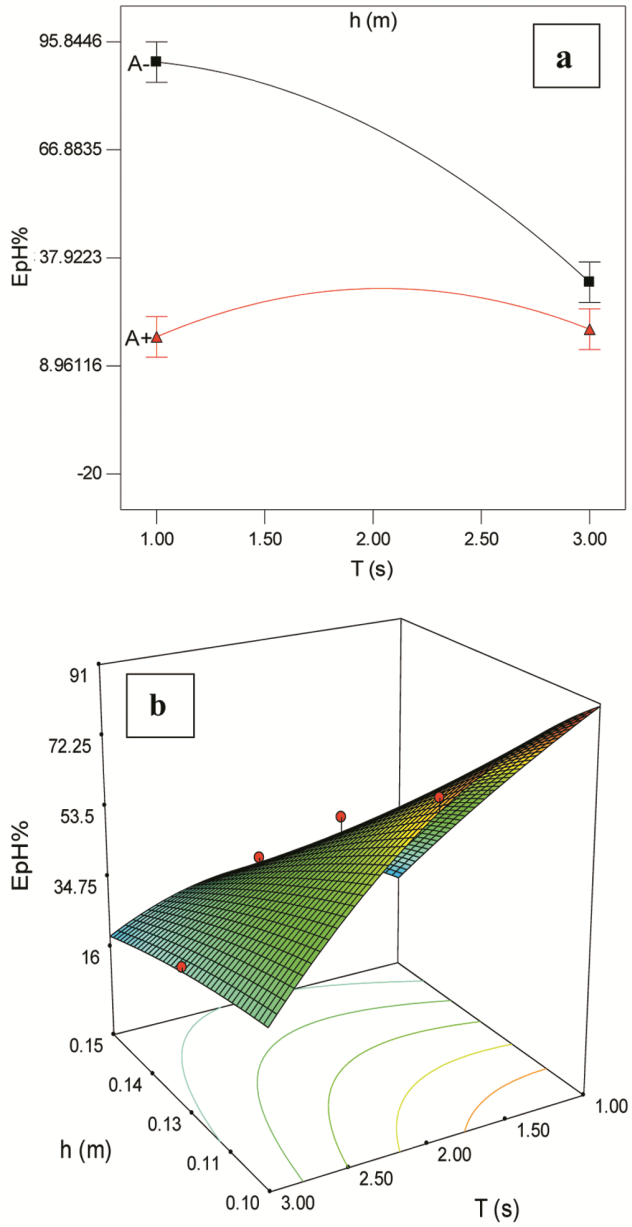

Fig. 5 — Interaction effect of h and T on E%: (a) two-way interaction effect, and (b) surface plot

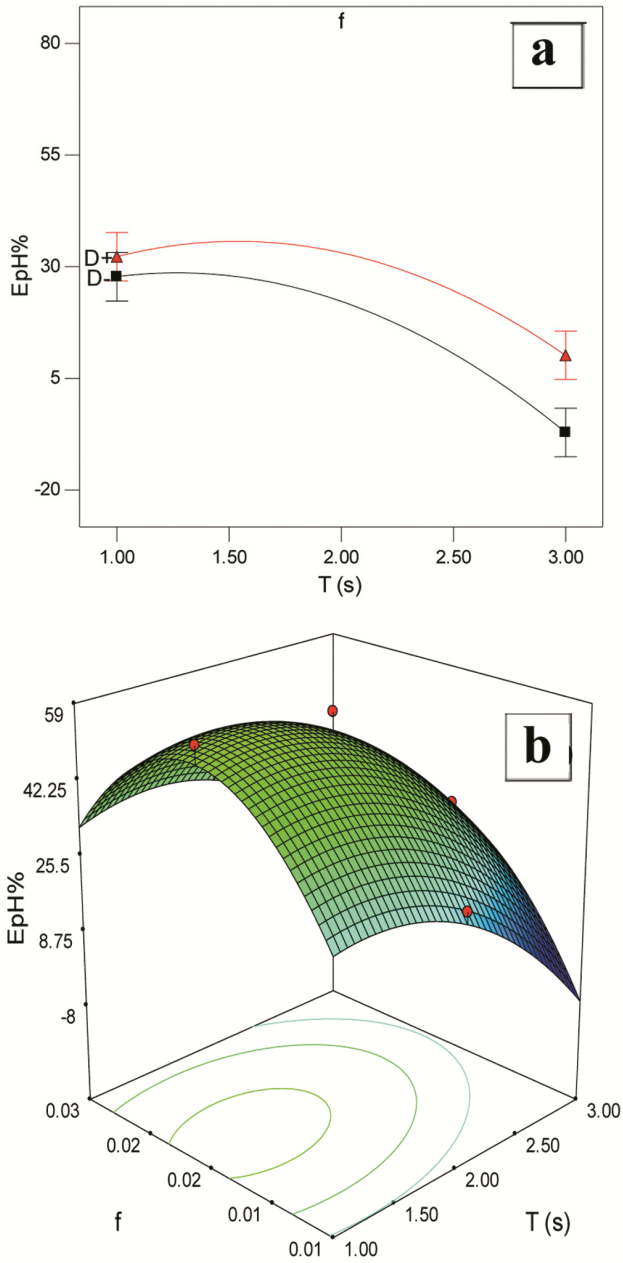

Fig. 6 — Interaction effect of T and f on E%: (a) two-way interaction effect, and (b) surface plot

vegetation zone, decreasing to as low as (23 %). E% rises with the wave period for small values of T to a point and reduces gradually for large values of T as it travels through the vegetation field. This may be attributed to larger changes in empirical wave loss coefficients for short peak wave phases, and strongly converging for longer T. Furthermore, the theoretical coefficients of the decay of the wave are found to be almost independent during variations from the peak times under dips.

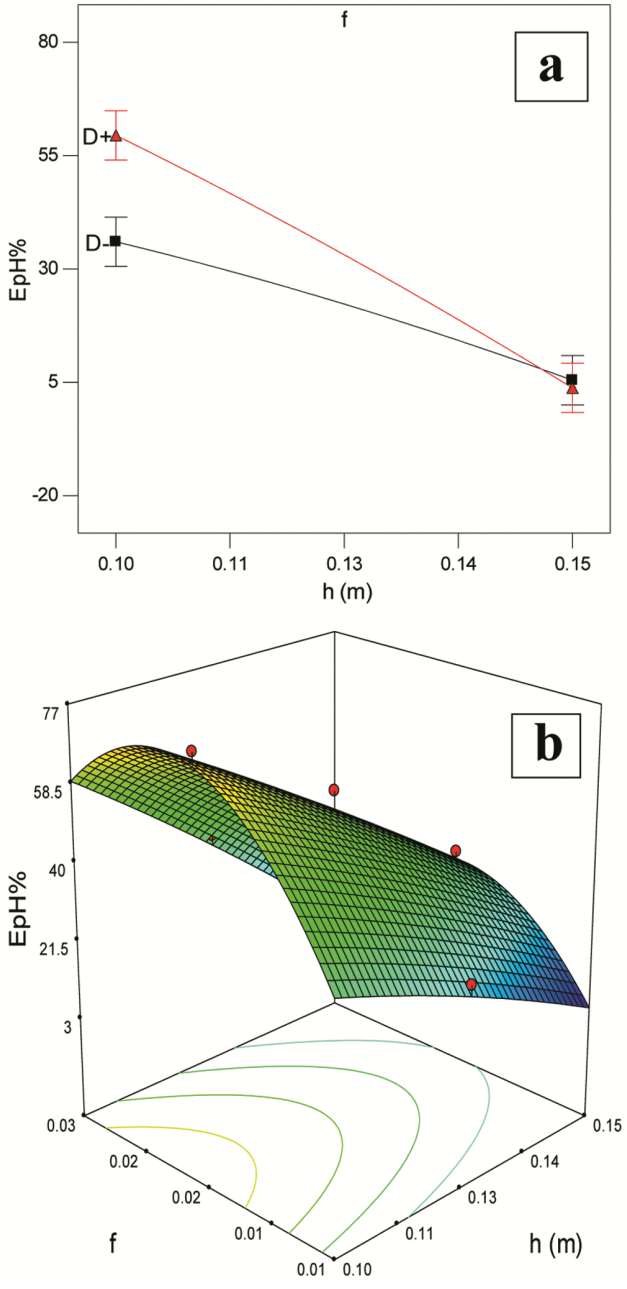

Fig. 7 — Interaction effect of h and f on E%: (a) two-way interaction effect, and (b) surface plot

Interaction effect of h and f

The map of interaction between two forms and the surface plot is shown in Figures 6(a & b) which demonstrate the effects of h and f on E%, at fixed T(2 s) and N (1353 stems/sq m), respectively. Although f alone has a positive effect on E% (Fig. 4D), the interaction between f and h has a negative effect. The relationship between h and f on the E% response surface plot (Fig. 6b) shows that an increase in f due to changes in bed roughness from steel to fine sand (statistically represented from -1 and 0) and from fine sand to coarse pebbles (statistically represented from 0 and +1) leads to an improvement in E%. When h has been at the lower level, the rise in roughness factor in the flume bed from 0.010 (surface flume of steel bed) to the flume of the pebbles bed (0.025) contributes to an increase between 40 to 60 % of E%. Nevertheless, an increase in h from 0.10 to 0.15 m under comparable circumstances causes a rise in E% to 5 % or less. Such findings explicitly indicate that water depth level has a more influential function in wave attenuation under test conditions relative to all other parameters considered in this experiment, which is in strong alignment with the results of the flow studies. The greater the water depth level over the canopy for unidirectional flow, the less effective it is to reduce the flood. The higher f and shallow h also allow greater wave-energy dissipation.

Interaction effect of T and f

There is also a statistically significant interaction effect (Table 3) on wave attenuation between T and f. Figures 7(a &b) display T and f interaction effects on E% along the vegetation meadow in a graphical way. Since the cumulative interaction effect is directly proportional to E%, an increase in T at minimum f (0.010) from 1 to 3 s induces a decrease of E%. Figure 7(b) also indicates that for all three different bed friction factors, shorter wave period (1 s) results in a higher percentage of wave energy reduction (73 %). However, the lowest f (0.010) at the longest wave period (3 s) is the lowest percentage (nearly zero) of wave energy reductions. In comparison, the mean f(0.025) results in a higher proportion of wave energy reduction in the shorter wave period (1 s). Of all other process control parameters considered in this study, the most contradictory results of the literature were the impact of wave period on dissipation. Möller et al.[19] stated that at all wave periods, salt marshes reduced wave energy by the same degree as flat sand low-flows. But other studies[16] indicated that vegetation-

based wave attenuation is primarily high-frequency high-wave dependent. Around 35 % of wave height dropped in the meadow owing to a decrease in wave duration. The inverse non-linear influence of the wave cycle on energy fluctuations (Fig. 7b) in the vegetation meadow is in strong alignment with the recorded findings[15].

Conclusion

Designed research and statistical comparison analysis to understand the influence of control parameters on wave attenuation output from the heterospecific aquatic seagrass meadow is presented. The experiments were carried out on a laboratory scale using three level-four core composite, face-centered surface response variables. Four control parameters, including wave period (T, 1, 2 and 3 s), water depth (h, 0.10, 0.125 and 0.15 m), bed roughness (f, 0.010, 0.017 and 0.025) and plant density (N, 543, 1353 and 2163 stems/sq m) were tested for the percentage of wave energy reduction (E%). A nonlinear analytical model was developed such that the model predictions were tested for comparison and validation against experimental results. All of the operating parameters, *i.e.* statistically relevant primary and interaction effects were analyzed and plotted on both-way interaction plots as well as 3D response surface plots. The findings showed that both individually and in combination under specified conditions, all of the parameters considered have major effects on wave energy attenuation. The results also verified that h has a negative linear main effect on E %, while N and f have a positive nonlinear effect, and T has a negative nonlinear effect. Water depth has the largest contribution to wave attenuation, as it has statistically significant two-way interactions with all the other three parameters (N, T, and f) although it does not individually have any nonlinear key effect. The RSM technique was found to be extremely effective for the prediction of heterospecific seagrass meadow wave energy reduction as the results of the variance analysis (ANOVA) suggested good agreement when comparing the experimental results with the model predictions at a high determination coefficient (R^2) of 0.9437 (with p-value < 0.05).

Acknowledgments

The authors would like to thank, for providing research facilities and encouragement, the Department of Civil Engineering, National Institute of Technology, Tiruchirappalli (NITT), Tamil Nadu, India.

Conflict of Interest

The authors state that there are no known conflicts of interest related to this research paper.

Author Contributions

Conceptualization and job layout: SH & RM. SH: Conceptualization, methodology, collection of data, research, data interpretation, software, and manuscript preparation. RM: The entire analysis, equipment, examination, and supervision of corrections of the manuscript.

References

1 Larkum A W D, Orth R J & Duarte C M (Eds.), Seagrasses: *Biology, ecology and conservation*, (Springer Netherlands), 2006, pp. 676.

2 Manca E, Cáceres I, Alsina J M, Stratigaki V, Townend I, et al., Wave energy and wave-induced flow reduction by full-scale model *Posidonia oceanica seagrass, Cont Shelf Res*, 50–51 (2012) 100–116.

3 Möller I, Kudella M & Rupprecht F, Wave attenuation over coastal salt marshes under storm surge conditions, *Nat Geosci*, 7 (2014) 727–731.

4 Specht A, Gordon I J, Groves R H, Lambers H & Phinn S R, Catalysing transdisciplinary synthesis in ecosystem science and management, *Sci Total Environ*, 534 (2015) 1–3.

5 Xu S, Liu Y, Wang X & Zhang G, Scale effect on spatial patterns of ecosystem services and associations among them in semi-arid area: A case study in Ningxia Hui Autonomous Region, China, *Sci Total Environ*, 598 (2017) 297–306.

6 Guannel G, Ruggiero P & Faries J, Integrated modeling framework to quantify the coastal protection services supplied by vegetation, *J Geophys Res Ocean*, 120 (2015) 324–345.

7 Vuik V, Suh Heo H Y, Zhu Z, Borsje B W & Jonkman S N, Stem breakage of salt marsh vegetation under wave forcing: A field and model study, *Estuar Coast Shelf Sci*, 200 (2018) 41–58.

8 Koch E W, Sanford L P, Chen S N, Shafer D J & Smith J M, Waves in seagrass systems: review and technical recommendations (No. ERDC-TR-06-15), 2006.

9 Luhar M & Nepf H M, Wave-induced dynamics of flexible blades, *J Fluids Struct*, 61 (2016) 20–41.

10 Feagin R A, Furman M & Salgado K, The role of beach and sand dune vegetation in mediating wave run up erosion, *Estuar Coast Shelf Sci*, 219 (2019) 97–106.

11 Koftis T & Prinos P, Estimation of wave attenuation over Posidonia Oceanica, *Appl Coastal Res*, 4 (2014) 1–8.

12 Bouma T J, De Vries M B & Low E, Trade-offs related to ecosystem engineering: A case study on stiffness of emerging macrophytes, *Ecology*, 86 (2005) 2187–2199.

13 Best Ü S N, Wegen M, Van Der, Dijkstra J, Willemsen P W J M, et al., Environmental Modelling & Software Do salt marshes survive sea level rise ? Modelling wave action, morphodynamics and vegetation dynamics, *Environ Model Softw*, 109 (2018) 152–166.

14 Mendez F J & Losada I J, An empirical model to estimate the propagation of random breaking and nonbreaking waves over vegetation fields, *Coast Eng*, 51 (2004) 103–118.

15 Stratigaki V, Manca E, Prinos P, Losada I J, Lara J L, et al., Large-scale experiments on wave propagation over Posidonia oceanica, *J Hydraul Res*, 49 (2011) 31–43.
16 Bradley K & Houser C, Relative velocity of seagrass blades: Implications for wave attenuation in low-energy environments, *J Geophys Res Earth Surf*, 114 (2009) 1–13.
17 Knutson P L, Brochu R A, Seelig W N & Inskeep M, Wave damping inSpartina alterniflora marshes, *Wetlands*, 2 (1982) 87–104.
18 Möller I & Spencer T, Wave dissipation over macro-tidal saltmarshes: Effects of marsh edge typology and vegetation change, *J Coast Res*, 36 (2002) 506–521.
19 Möller I, Spencer T, French J R, Leggett D J & Dixon M, Wave transformation over saltmarshes: a field and numerical modelling study from North Norfolk, England, *Estuar Coast Shelf Sci*, 49 (1999) 411–426.
20 Augustin L N, Irish J L & Lynett P, Laboratory and numerical studies of wave damping by emergent and near-emergent wetland vegetation, *Coast Eng*, 56 (2009) 332–340.
21 Hu Z, Suzuki T, Zitman T, Uittewaal W & Stive M, Laboratory study on wave dissipation by vegetation in combined current-wave flow, *Coast Eng*, 88 (2014) 131–142.
22 Vuik V, Jonkman S N, Borsje B W & Suzuki T, Nature-based flood protection: the efficiency of vegetated foreshores for reducing wave loads on coastal dikes, *Coast Eng*, 116 (2016) 42–56.
23 Vuik V, van Vuren S, Borsje B W & van Wesenbeeck B K, Assessing safety of nature-based flood defenses: Dealing with extremes and uncertainties, *Coast Eng*, 139 (2018) 47-64.
24 Koftis T, Prinos P & Stratigaki V, Wave damping over artificial Posidonia oceanica meadow: A large-scale experimental study, *Coast Eng*, 73 (2013) 71–83.
25 Suzuki T, Zijlema M, Burger B, Meijer M C & Narayan S, Wave dissipation by vegetation with layer schematization in SWAN, *Coast Eng*, 59 (2012) 64–71.
26 Tang J, Shen S & Wang H, Numerical model for coastal wave propagation through mild slope zone in the presence of rigid vegetation, *Coast Eng*, 97 (2015) 53–59.
27 Anderson M E & Smith J M, Wave attenuation by flexible, idealized salt marsh vegetation, *Coast Eng*, 83 (2014) 82–92.
28 Manca E, Stratigaki V & Prinos P, Large scale experiments on spectral wave propagation over *Posidonia oceanica seagrass, In: Environmental Hydraulics*, (CRC Press), 2010, pp. 463-468.
29 Jadhav R S, Chen Q & Smith J M, Spectral distribution of wave energy dissipation by salt marsh vegetation, *Coast Eng*, 77 (2013) 99–107.
30 Paquier A E, Haddad J, Lawler S & Ferreira C M, Quantification of the Attenuation of Storm Surge Components by a Coastal Wetland of the US Mid Atlantic, *Estuaries Coasts*, 40 (2017) 930–946.
31 Marsooli R & Wu W, Numerical investigation of wave attenuation by vegetation using a 3D RANS model, *Adv Water Resour*, 74 (2014) 245–257.
32 Luhar M & Nepf H M, Wave-induced dynamics of flexible blades, *J Fluids Struct*, 61 (2016) 20–41.
33 Paul M, Rupprecht F, Möller I, Bouma T J, Spencer T, et al., Plant stiffness and biomass as drivers for drag forces under extreme wave loading: A flume study on mimics, *Coast Eng*, 117 (2016) 70–78.
34 Jagtap T G, Komarpant D S & Rodrigues R, The Seagrasses of India, In: *World Atlas of Seagrasses*, edited by E P Green & F T Short, (University of California Press, Berkeley Los Angeles London), 2003, pp. 101–108.
35 Kobayashi N, Raichle A W & Asano T, Wave attenuation by vegetation, J Waterway, Port, Coastal, Ocean Eng, 119 (1) (1993) 30–48.
36 Dalrymple R A, Kirby J T & Hwang P A, Wave Diffraction Due to Areas of Energy Dissipation, J Waterw Port Coastal Ocean Eng, 110 (1984) 67–79.
37 Mullarney J C & Henderson S M, Wave-forced motion of submerged single-stem vegetation, *J Geophys Res Ocean*, 115 (2010) 1–14.
38 Fonseca M S & Cahalan J A, A preliminary evaluation of wave attenuation by four species of seagrass, *Estuar Coast Shelf Sci*, 35 (1992) 565–576.
39 Kuo J & den Hartog C, Taxonomy and Biogeography of Seagrasses, In: *Seagrasses: Biology Ecology and Conservation*, (Springer, Netherlands), 5 (2006), pp. 1–23.
40 El Shaffai A, *Field Guide to Seagrasses of the Red Sea*, 1st edn, edited by A Rouphael & A Abdulla, (Gland, Switzerland: IUCN and Courbevoie, France: Total Foundation), 2011, pp. viii+56. https://portals.iucn.org/library/sites/library/files/documents/2011-057.pdf
41 Montgomery D C & Runger G C, Applied Statistics and probability for engineers, *Eur J Eng Educ*, 19 (3) (1994) pp. 83